Research for thermal load and procedure to predict fatigue life up to form a fatigue crack on CFRP/Aluminium hybrid joints

Takao Okada[1], Hisashi Kumazawa[2], Takafumi Toyosawa[2], Tomo Takeda[2], Toshiyuki Kasahara[3], Koichi Yamada[2], Kasumi Nagao[2], Yuichiro Aoki[2] and Hirokazu Shoji[2]

[1] Japan Aerospace Exploration Agency, okada.takao@jaxa.jp
[2] Japan Aerospace Exploration Agency
[3] Adecco Group Japan

Abstract: The research to evaluate the fatigue life up to form a fatigue crack in a metal/composite hybrid joint has been conducted. Thermal stress at high and low temperature is occurred in metal/composite hybrid joints due to the difference of thermal expansion between metal and composite materials. Accurate calculation of stress and strain in the joint including thermal effect is applied to SWT (Smith-Watson-Topper) equation for prediction of the fatigue life of the metal/composite hybrid joints. In this study, thermal load in a mechanically fastened hybrid joint under temperature cycle was investigated experimentally and numerically. In addition, material constants of aluminum sheets were obtained with the strain-controlled fatigue tests for precise prediction by SWT equation.

For the investigation of the thermal load in the hybrid joint, the mechanically fastened hybrid joint specimens composed of two aluminum plates and a composite plate were prepared. Experimental results indicated that relationships between temperature and elastic strain on specimen surface in temperature cycle exhibit hysteresis loop. Finite element analysis for the hybrid joint was also conducted and captured the hysteresis loop obtained by the experiment.

In the material data measurements, the fatigue life for the aluminum alloy in relation to the product of the strain amplitude and the maximum stress has been obtained by the strain-controlled fatigue tests. The strain-controlled fatigue tests are terminated when applied load is reduced by the fatigue crack. The obtained cycles are planned to evaluate the life for formation of certain crack size represented by the applied load reduction to 95% of the maximum load, and the relationship between the crack formation cycles and the product of the maximum stress and the strain amplitude are obtained. The obtained relationship would be used to preliminary predict a fatigue crack formation life of the hybrid joint using FEM result.

Keywords: Hybrid joints, Thermal load, SWT equation, FEM

INTRODUCTION

WFD (Widespread Fatigue Damage) involves the simultaneous presence of multiple cracks, at multiple locations, that are of sufficient sizes and density. And then in case the tensile fatigue load is applied to the structure with WFD, the structure will no longer meet the residual strength requirement. Many research activities for multiple fatigue crack have been conducted [1-4], because the prediction

of those crack growth is impractical using deterministic linear elastic fracture mechanics. FAA (Federal Aviation Administration) amends the CFR (Code of Federal Regulation) in 2011 and the current requirement demands to evaluate the possibility of the WFD to the metal structure under tensile fatigue loading for transport category aircraft [5]. FAA also issue the guideline for WFD [6].

The LOV (Limit of Validity) is the period of time (in flight cycles, flight hours, or both), up to which it has been demonstrated that WFD is unlikely to occur in an airplane structure by virtue of its inherent design characteristics and maintenance actions. WFD average behavior is defined as the period of the time, without intervention, 50% of the fleet is expected to have developed WFD during operation. Therefore, LOV has to be shorter than the WFD average behavior. Determination of the LOV is based on the experiment, operational experience and result of the teardown inspection. The result of the full scale fatigue test is usually employed to evaluation of the LOV.

Same as the aircraft structure using metallic material, the hybrid joint composed of the metal and CFRP (Carbon Fiber Reinforced Plastics) also have to be evaluated for the susceptibility of the WFD, in case its metal part carries the fatigue load. Because the thermal expansion is different between the metal and the CFRP, evaluation of WFD susceptibility have to be based on not only the external load but also the thermal load caused by the thermal experience during operation. And the corresponding LOV should include the effect of thermal load. Because the test speed of the thermal load is quit slow comparing to the external load, the period for WFD evaluation under thermal load seems to be time consuming comparing to that under external load.

In 2015, ARAC (Aviation Rulemaking Advisory Committee) assigned TAMCSWG (Transport Airplane Metallic and Composite Structures Working Group) under TAE (Transport Airplane and Engine) Subcommittee in order to provide advice and recommendation on amendment of damage tolerant requirement in CFR and preparation of related guidance material. TAMCSWG proposes recommendations to apply the analysis supported by test evidence to WFD evaluation of hybrid joint [7]. Followings are included in recommendations. Attempts to simulate the self-balancing thermal loads by an increase in mechanical loads in full scale tests is not acceptable since the resulting total loads will not adequately represent internal load distributions. Simulation of certain loading conditions in the full-scale testing is not necessary, if it can be shown impractical and accurately addressed by analysis supported by test evidence. For damage tolerance evaluation of metallic structure, certain loads, such as thermal fatigue loads, will use analysis supported by test evidence, typically with lower level test articles (e.g., component, sub-component, and coupons). For demonstration of freedom from WFD, the particular loads, which cannot be applied in the full-scale fatigue test (e.g., thermal effect), can be incorporated in the existing acceptable means of compliance-- that is, a combination of crack growth analysis and a tear down inspection. Fatigue test including cyclic thermal load is time consuming comparing to that for external load and then development of analytical procedure for thermal load is desired.

In 2010s, NRCC (National Research Council Canada) and JAXA (Japan Aerospace Exploration Agency) conducted collaborative research work for WFD evaluation of a riveted lap joint [4]. The fatigue life up to first link-up of the adjacent cracks on the riveted lap joint was predicted using stress, strain and fatigue test result of the riveted lap joint including crack growth data, SWT equation [8], Global – Local FEM including the effect of fastening process and external cyclic loading and probabilistic crack growth analysis using CanGROW. The rate of CFRP on aircraft structural weight has been increasing in several decades. JAXA have been conducted the research to evaluate the fatigue life up to form a fatigue crack at certain size in a metal/composite hybrid joint.

This paper presents the review results how to use former collaborative research work to current research for hybrid joint and current status for experimental test and numecircal simulation.

EVALUATION PROCEDURE

WFD evaluation procedure for riveted joint

NRCC and JAXA conducted the research work for WFD prediction of riveted lap joint. Two Aluminium plates with 1.25 mm thick are fastened by 3 rows of 20 rivets. It features the fuselage lap joint which is one of the WFD-susceptible structure of an aircraft. Fatigue test of the riveted joint is

conducted until the final failure of the specimen. Strain distribution on the joint is measured using the strain gauges and crack growth behaviour are observed at a periodic interval. Fracture surface observation is also conducted in order to identify shape and type of fatigue cracks and to evaluate the fracture origin. From the analytical point of view, global – local FEM analysis is conducted. The effect of rivet squeezing process and external load on riveted joint are calculated by the FEM and maximum stress and strain amplitude at the critical location are obtained. The fatigue life to form 0.5mm crack is predicted substituting these values into SWT equation which exhibit the relation between fatigue life and product of maximum stress and strain amplitude. It considers the effect of mean stress on fatigue life of the material.

$$\sigma_{max}\ \frac{\Delta\varepsilon}{2} = \frac{\left(\sigma_f'\right)^2}{E}\left(2\,N_f\right)^{2b} + \sigma_f'\,\epsilon_f'\left(2\,N_f\right)^{(b+c)} \tag{1}$$

σ'_f: coefficient of fatigue limit, ε'_f: coefficient of plastic fatigue strain, E : Young's Modulus
b : fatigue strength exponent, c : fatigue ductility exponent, N_f: Number of load cycles

σ'_f, ε'_f, b and c are the material data obtained by the coupon tests. In the collaborate research work, these material data in other paper are used. N_f is the life of the coupon and it is defined as a fatigue life to form 0.5 mm crack. EIFS (Equivalent initial flaw size) distribution is prepared and NRCC's in-house code, CanGROW, is employed for preliminary Monte Carlo simulation using an EIFS distribution, and then produced a fatigue life distribution to the first link-up. The collaborate research work identifies that the critical location is around the rivet hole and the rivet squeezing force, interference fit between rivet hole and rivet shank and coefficient of friction affect the stress and the strain at the critical location. In addition, the stress and the strain obtained by the FEM analysis could be used to predict the fatigue life of the riveted joint.

Fatigue origin of the hybrid joint on WFD scenario is considered as the edge of the fastener hole affected by the stress concentration at the hole and fretting at the faying surface, based on the discussion to aircraft manufacturer. Thus, fracture origin and factor affecting its formation are same between riveted joint and metal/CFRP hybrid joint. It suggests that the WFD evaluation procedure for riveted joint proposed by NRCC and JAXA would be applicable to that for metal/CFRP hybrid joint. CFRP in this case has the orthotropy and this causes additional calculation cost. However, evaluation of rivet fastening requires the modeling of the finite deformation of the rivet and the plate, and re-mesh of the region. This would cause high penalty for numerical validity and calculation cost. It means that the technical difficulty for WFD evaluation of hybrid joint might be less comparing to that for conventional riveted joint. Figure 1 shows the flow chart for the proposed procedure. In figure 1, a circumferential fuselage joint is selected as the candidate location where the hybrid joint is applied. The flow chart consists of the development of fatigue life prediction curve, the validation of FEM model and the evaluation of stress and strain of hybrid joint under thermal and external load. The fatigue life prediction curve is obtained by the coupon test result as shown in the left part in figure 1. The FEM model for thermal load is validated by comparison between experimental and numerical results. The validated model is used for the evaluation of stress and strain of hybrid joint under thermal and external load as shown in the right part in figure 1. These data are substituted in the SWT equation and the fatigue life is predicted as shown in the bottom part in figure 1.

Experimental procedure for material data used for SWT equation

This section describes the procedure to obtain experimental results used for the materials data substituted in the fatigue life prediction curve shown in figure 1. The material data used for prediction of 0.5 mm crack on riveted joint is described in ref. 8. The data were obtained by the round specimen with 4 mm diameter machined from the 4.8mm thick plate. Unfortunately, the data in ref. 8 does not include the test data for lower strain range and the life between 30,000 and 100,000 cycles corresponding to the LOV for regional jet. In this research, we conducted coupon test in order to obtain the material data. The dimension of the specimen is shown in figure 2. The thickness is 3.175 mm and the width of the gauge section is 3 mm. Same as ref. 8, strain-controlled fatigue test is conducted. Hydraulic fatigue test equipment 8802 (100kN), manufactured by Instron, is used for the test. Extensometer 2630-120

with 8 mm gauge length is attached to the specimen. Strain amplitudes are 0.8, 0.6, 0.4, 0.3 and 0.25 %, and mean strain is 0.0 (R_ε=-1). Test speed is 0.2 Hz, because strain is controlled by extensometer. Test waveform is sine shape. The specimen setup is shown in figure 3. In order to terminate the coupon test before final failure, test machine is set to stop, in case the maximum load at a cycle decreases apparently comparing to the maximum load at the stable period during the test. After the test is terminated, the cycle when maximum load decreases to 95% of the maximum load at the stable period is defined as the life used for evaluation.

Experimental procedure to evaluate strains by thermal cycles on hybrid joint

This section describes the procedure to obtain experimental results used for the validation of FEM model concerning about the thermal load shown in figure 1. The fuselage section joined between metal and CFRP is selected as the candidate part and specimen geometry is proposed by the aircraft manufacturer. In general, GFRP is attached to the surface on the CFRP to prevent the galvanic corrosion. In this research, the main purpose is to evaluate the effectiveness of the proposed procedure. GFRP is not applied in this research, because it would not affect the thermal load evaluation. The dimension of the Aluminium/CFRP hybrid joint is shown in figure 4. Prepreg used for CFRP is Toray T800S/3900-2B and stacking sequence is $[45/0/-45/90]_{3s}$. Nominal thickness of the CFRP plate is 4.56 mm. 2024-T3 Aluminium plate with the thickness of 2 mm is used for the hybrid joint. The dimension of the fastener hole is between 4.826 and 4.902 mm (0.190 and 0.193 inch). The Hi-Lite fasteners composed of HST10-6-6 pin and HST79CY6 collar are used. The fastening torque is set between 2.83 and 3.96 Nm (25 and 35 inch-pound) which is recommended by supplier.

The thermal shock chamber, TSD-100, manufactured by ESPEC Co., shown in figure 5 is used for temperature control. The equipment consists of top chamber for high temperature (between 60 and 320 degrees Celsius) and bottom chamber for low temperature (between -77 and 0 degrees Celsius). The specimen moves between these chambers.

The temperature in the specimen, strain on surface and out of plane deformation are measured and specimens are prepared for each purpose as shown in figure 6. Temperature on the Aluminium plate, in CFRP and in chamber are measured using type K thermocouples as shown in figure 6 (a). The thermocouple in CFRP is impregnated at the centre of the specimen during the manufacturing of the CFRP. Strains on the Aluminium plate are measured using tri-axial strain gauges. FRAB-2-11, made by Tokyo Measuring Instruments Laboratories Co., Ltd., is used for evaluation. The strain gauges are located at the centre of four fasteners as shown in figure 6 (b). As shown in the figure, 0 and 90 degrees correspond to the directions along long side and short side, respectively. Measured strain on the Aluminium alloy is composed of the thermal strain and the elastic strain as shown in equation (2) as follows:

$$\epsilon_t = \epsilon_{th} + \epsilon_e \tag{2}$$

ε_t: Strain measured by strain gauge, ε_{th}: Thermal strain, ε_e: Elastic strain
In this research, thermal strain, ε_{th}, is measured using unassembled Aluminium specimen. The elastic strain in Aluminium alloy is obtained using the strain on hybrid joint and that on Aluminium alloy as single unit.

$$\epsilon_{e(j)} = \epsilon_{t(j)} - \epsilon_{th(al)} \tag{3}$$

The subscript, *j* and *al*, means the hybrid joint and Aluminium alloy as single unit, respectively.

The out of plane deformation of the Aluminium plate is measured in the area shown in figure 6 (c), using the wide area three-dimensional measurement system controller VR-3000, manufactured by KEYENCE. The measurement accuracy is 2.5 μm. The specimen is set to the chamber and is exposed to the objective temperature. Although out of plane deformation is measured outside of the chamber, the specimen temperature during measurement is confirmed by thermocouple on the specimen.

Numerical simulation to evaluate stress and strain by thermal cycles on hybrid joint

This section describes the procedure to obtain numerical results used for the validation of FEM model concerning about the thermal load shown in figure 1. In order to evaluate the effect of temperature change on stress and strain in the specimen shown in figure 4, a quarter of the specimen is modelled as shown in figure 7. Origin of the coordinate is located at the middle of the specimen and x, y and z directions correspond to directions along long side, short side and through the thickness direction, respectively. The commercial FFM software, ABAQUS 2019, is employed for the numerical simulation. The element C3D8 (8 nodes and 6 surfaces) is used in the FEM model. In this model, the pin and the collar are modelled as one part. The boundary between fasteners, Aluminium plates and CFRP plates are modelled as contact surfaces and the coefficient of friction is set to 0.2 for all of contact surfaces. The average dimension is applied to the shank of the fastener and the hole diameter. Fastening force is set to 3559 N (800 lbs) based on the supplier datasheet. The developed FEM model is shown in figure 8.

The CFRP plate is treated as the homogeneous orthotropic elastic body because the stacking sequence of the plate is quasi-isotropic. Aluminium plate, and the pin and the collar made by Titanium alloy are treated as the elastic body. The temperature dependence to the material properties is considered in this model. The material property of the unidirectional CFRP for each temperature is based on the data in the references [9, 10] and the material properties of the quasi-isotropic CFRP are calculated using the material properties of the unidirectional CFRP. Figure 9 shows the effect of temperature on material properties of the quasi-isotropic CFRP. The subscripts 1, 2 and 3 correspond to 0 degree, 90 degrees and through the thickness directions, respectively. The coefficient of thermal expansion of the unidirectional CFRP is based on the data in ref. 9 and that of quasi-isotropic CFRP is calculated. The material properties in MMPDS [11] are used for those of Aluminium alloy and Titanium alloy.

RESULTS

Strain controlled test result used for SWT equation

Figure 10 shows the relationship between strain amplitude and fatigue test cycles together with the data in ref. 8. In the figure, the data “terminated” means that the data in case the fatigue test is terminated by the load decrease and the data “N 0.95” means that the data obtained as the maximum load decrease to 95 % of the Maximum load at the stable period. Although the data in ref. 8 seems to run out in case strain amplitude is above 0.35, the specimen in this test occures the fatigue crack for lower strain amplitude. The tested specimen in ref. 8 grinded out from the thick plate and refined particle on the surface is removed. Basically the refined particles increases the fatigue life, the edge of the specimen causes to decrease the fatigue life. The cycles to terminate the test for 0.25 strain amplitude are between 120,000 and 190,000 cycles and it covers the required life. The vertical axis in figure 11 indicates the product of the maximum stress and the strain amplitude at the stable period. The product is used for the SWT equiation. It is considered that the scatter of the graph become narrow by incorporating the effect of maximum stress. The elastic and the plastic strain amplitude are also obtained from the experimental data and then the parameters used in the SWT equation are evaluated from the test data. Evaluted parameters are shown in table 1. The relationship between all of strain amplitude and fatigue cycle are shown in figure 12. Lines are drawn using the parameter in table 1 and plots indicate the test result. The horizontal axis corresponds to the twice as the fatigue cycles when maximum load decreases to 95 % of the maximum load at the stable period. The obtained plastic strain is much lower compaing to the elastic strain in this research.

Experimental result for strains by thermal cycles on hybrid joint

The variation of the specimen temperature during heating and cooling are measured preliminary. Until 1,000 seconds after the chamber start to change the temperature, the difference of the specimen temperature converges within 1 degree Celsius. Based on the results, strain measurement is conducted at 1,000 seconds after the temperature in the chamber is controlled to objected temperature.

Figure 13 shows the elastic strain changes during temperature cycle. The temperature in cycle starts at 25 degrees Celsius and is heated up to 85 degrees Celsius, cooled down to -55 degrees Celsius and go back to 25 degrees Celsius. The figure identifies that the elastic strain changes nonlinearly around the peak temperature, irrespective to the strain gauge location. In addition, irrespective to strain gauge location, strain variation along 0 degree is largest comparing to other directions and it is larger for the gauge located close to the centre of the specimen. It is because the boundary of the gauge 1 to 0 degrees direction is not fastened and the elastic strain seems to be less restricted. Stain variation along 90 degrees is the smallest and about 300 με, irrespective to strain gauge location. It is because that the boundary to 90 degrees direction is same for all strain gauges.

Out of plane deformation of the Aluminium plate at 25 degrees Celsius, about 85 degrees Celsius and -55 degrees Celsius are shown in figure 14. In the measurement, nominal height of four fastener head is defined as 1.27 mm and upward deformation is treated as positive. Although, the predefined torque is applied at the room temperature, the specimen surface is not flat at room temperature. At room temperature, Aluminium plate around fastener hole become convex because of the fastening force and therefore the surface at the middle of four fasteners locates relatively upward. At -55 degrees Celsius, Aluminium plate is thermally contracted comparing to the CFRP and it decreases out of plane deformation. At 85 degrees Celsius, out of plane deformation becomes larger vice versa.

Numerical results for stress and strain by thermal cycles on hybrid joint

Figure 15 shows variation of the strain obtained by FEM along 0 degree during three thermal cycles. Figure 15 indicates that the nonlinear behaviour of the stain variation seems to be observed, when temperature reaches room temperature. In addition, it is found that strain variation to temperature is close irrespective to the number of the thermal cycles, after temperature increase at first cycle. This feature is observed not only for other gauge directions but also for other gauge locations. It is confirmed that variation of stresses and strains after second thermal cycles are mostly identical, variation of stresses and strains at second thermal cycles are used to compare those for experimental results. The numerical results are also shown in figure 13 together with the experimental result. In the figure, strains at room temperature in the beginning of second thermal cycles in the numerical simulation is set to zero, because those in the experiment is set to zero at room temperature after several thermal cycles.

Material nonlinearity is not considered in this numerical simulation. Nonlinearity of strains to temperature is caused by the thermal dependence of material property and friction between the materials. And hysteresis of strains to temperature is affected by friction between the materials.

In numerical simulation, strain variations along 90 degrees direction at each gauge location are close each other. On the other hand, strain variations along 0 degrees direction at gauge one is smallest, while those at gauge two and gauge three are similar. As described in the previous section, strain constraint at gauge one is less comparing to others and then it becomes smaller. Scatter for fastening force caused by fastener size itself and scatter for the coefficient of friction based on surface roughness would affect quantitative evaluation.

Although the numerical results are similar to the experimental results qualitatively, there exists the difference between the numerical and the experimental result, quantitatively. Variation of fastening force based on the difference of fastener itself and that of friction force based on the difference of contact condition would affect this quantitative difference.

Figure 16 shows the strain distribution on Aluminium plate at z=2.28 mm where upper Aluminium plate contact to CFRP for second thermal cycle. At the hole edge where intersecting to y-direction, the elastic strain along x-direction is positive, irrespective to the temperature. This is because specimen around fastener hole is convex because of the fastening and it causes local bending of the Aluminium plate, as described in this section. It is confirmed that strain is negative at the corresponding location on the outer surface of the Aluminium alloy, where z=4.28 mm. The elastic strain is an order of 100 με and then elastic strain at the edge of the fastener hole is one order larger than the strain away from the hole. In addition, the strain at the fastener edge intersecting y-direction is the largest on the fastener hole away from the centre of the specimen in case the temperature is 85 degrees Celsius, while it is the smallest in case the temperature is -55 degrees Celsius.

Figure 17 shows the stress distribution on Aluminium plate at z=2.28 mm for second thermal cycle. Because of the local Aluminium plate bending at the fastener hole, stress along x-direction is positive

at the hole edge where intersecting to y-direction, irrespective to the temperature. The stress at the fastener edge intersecting y-direction is the largest on the fastener hole away from the centre of the specimen in case the temperature is 85 degrees Celsius, while it is smallest in case the temperature is -55 degrees Celsius. These features correspond to the strain distribution described at above sentence. The obtained maximum stress at the hole edge away from the centre of the specimen marked in figure 17 is 158 MPa and its range is 84 MPa, as shown in figure 18. It is confirmed that the peak stress does not occur at peak temperature. One of the maximum stresses planned for fatigue test is about 100 MPa and its stress ratio is 0.1. The detailed evaluation is planned to be conducted using the fatigue test specimen.

CONCLUSIONS

The procedure to evaluate the life of fatigue crack formation in the CFRP/metal hybrid joint under thermal and external load is proposed based on the evaluation procedure for WFD on riveted lap joint. The maximum stress and the strain amplitude at critical location of the hybrid joint obtained by FEM are transmitted to the SWT equation obtained by the coupon test and the fatigue cycle is predicted. Coupon test is conducted and material parameter used for SWT equation is obtained. In addition, thermal test is conducted to CFRP/Aluminium hybrid joint supposed to use at the fuselage joint in order to evalutate thermal stress and strain behavior and to develop the FEM model. The test result shows the hysterisis between temperature and the elastic strain. FEM result identifies that the friction between CFRP and Aluminium plate would cause the hysterisis. Obtained thermal stress is about 100 MPa and is same order of one of the external stress planned for the fatigue test of the hybrid joint and then the thermal stress would affect the fatigue cycles to form the fatigue crack and WFD behavior of the hybrid joint.

ACKNOWLEDGMENTS

The authors acknowledge to Mr. Toshiyasu Fukuoka et. al. at Mitsubishi Heavy Industries for the discussion about TAMCSWG activities and their comment to this research. The authors also thanks to Dr. Kenta Yamagiwa at National Institute of Occupational Safety and Health, Japan and Kobe Material Testing Laboratory Group for their comment to strain-controlled fatigue test.

REFERENCES

[1] R. P. G. Muller, An Experimental and Analytical Investigation on the Fatigue Behaviour of Fuselage Riveted Lap Joints, Delft University of Technology, Delft, Netherlands, 1995.
[2] J. Bakuckas, Jr., Full-Scale Testing and Analysis of Fuselage Structure Containing Multiple Cracks, DOT/FAA/AR-01/46, Final Report, Federal Aviation Administration, July 2002.
[3] H. Terada, T. Okada and P. Dybskiy, Effect of Load Components on Fatigue Like of Fuselage Model Structure, Proceedings of the International Committee on Aeronautical Fatigue 2001, Volume I, pp.263-272.
[4] G. Li, G. Renaud, M. Liao, T. Okada and S. Machida, A methodology for assessing fatigue life of a countersunk riveted lap joint, Advances in Aircraft and Spacecraft Science, Vol. 4, No. 1, 2017, pp. 1-19.
[5] FAA, Aging Airplane Program: Widespread Fatigue Damage: Federal Register Rules and Regulations 75 (219), 69746-69789.
[6] FAA, Establishing and Implementing Limit of Validity to Prevent Widespread Fatigue Damage, 2011.
[7] Transport Airplane Metallic and Composite Structures Working Group, Transport Airplane Metallic and Composite Structures Working Group – Recommendation Report to FAA, Final, 2018.
[8] C. Boller, T. Seeger, Materials Data for Cyclic Loading, Part D: Aluminum and Titaninum alloys, p.108-111
[9] S. Seki, et. al., Evaluation of fatigue life of thick CFRP laminates with toughened interlaminar

layers in out-of-plane and in-plane transverse directions, Transaction of the JSME (in Japanese), vol. 83, No. 851, No.16-00471, 2017,
[10] T. Morimoto et. al., JAXA Advanced Composites Database (Revised), JAXA Research and Development Memorandum, JAXA-RM-17-004, 2018, (in Japanese).
[11] MMPDS. Metallic Materials Properties Development and Standardization MMPDS-10. Federal Aviation Administration, USA, 2015.

Table 1: STW parameter evaluated from test results

σ'_f : coefficient of fatigue limit	1279 MPa
ε'_f: coefficient of plastic fatigue strain	0.118
b : fatigue strength exponent	-0.154
c : fatigue ductility exponent	-0.687

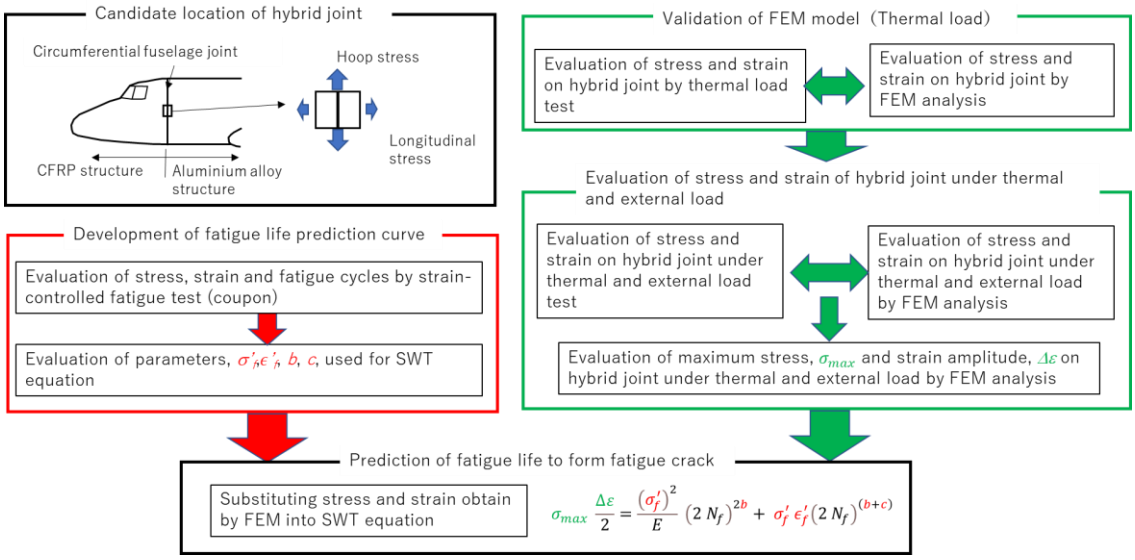

Figure 1: Flow chart for fatigue life prediction up to form fatigue crack in hybrid joint under thermal and external load

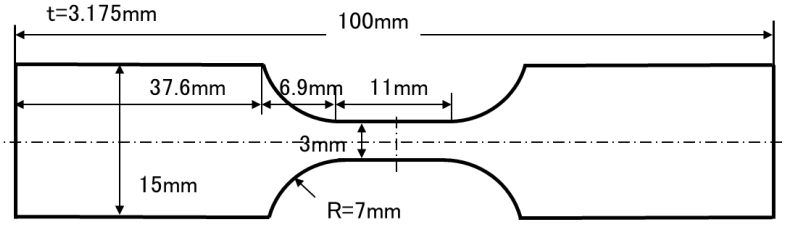

Figure 2: Strain controlled fatigue test specimen

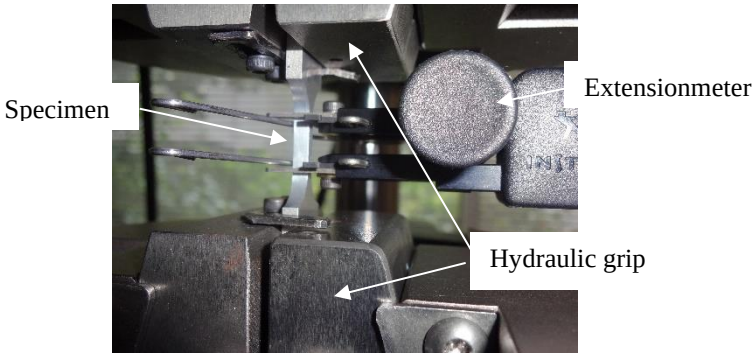

Figure 3: Test setup

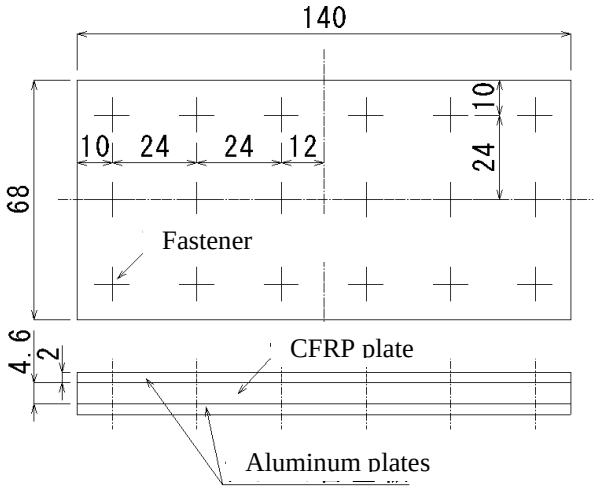

Figure 4: CFRP/Aluminium alloy hybrid joint specimen

Figure 5: Thermal shock chamber used for the temperature controlled test

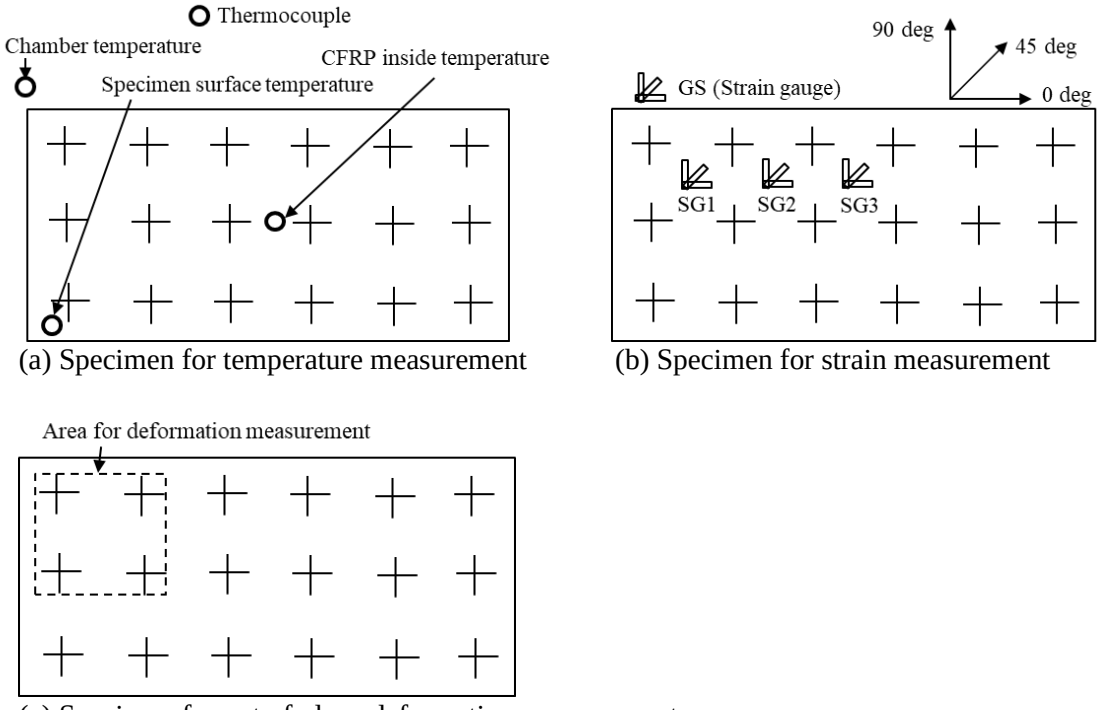

(a) Specimen for temperature measurement (b) Specimen for strain measurement

(c) Specimen for out of plane deformation measurement

Figure 6: Location of strain gauge and thermocouple

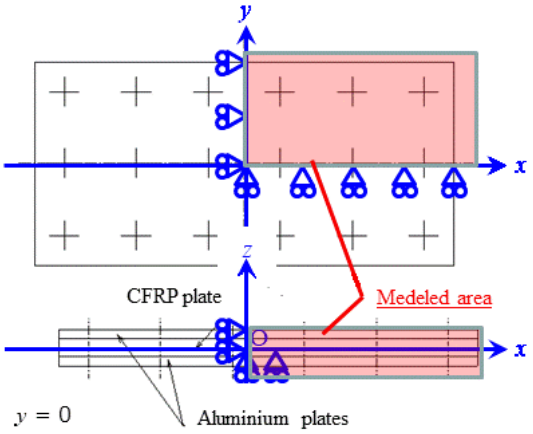

Figure 7: Area of FEM model

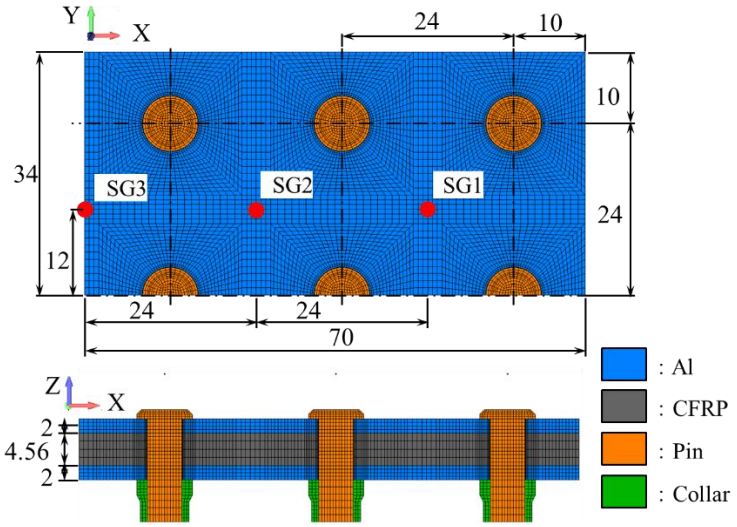

Figure 8: FEM model of the CFRP/Aluminium hybrid joint

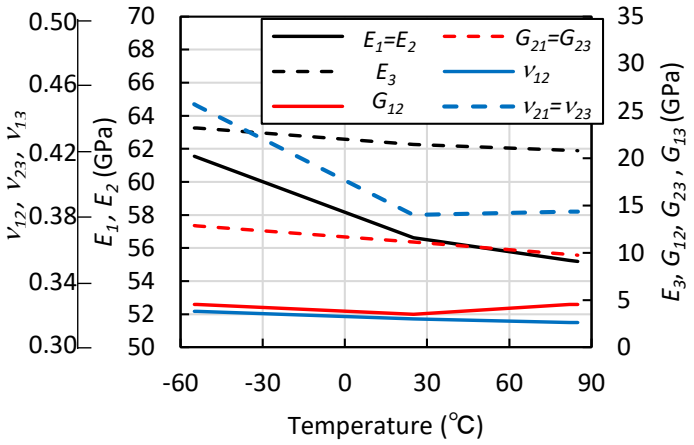

Figure 9: Effect of temperature on the material properties for quasi-isotropic CFRP (T800S/3900-2B)

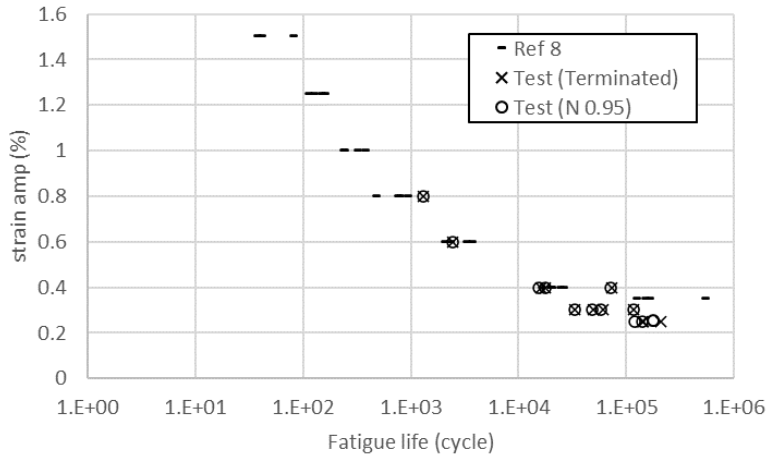

Figure 10: Relationship between strain amplitude and fatigue cycles

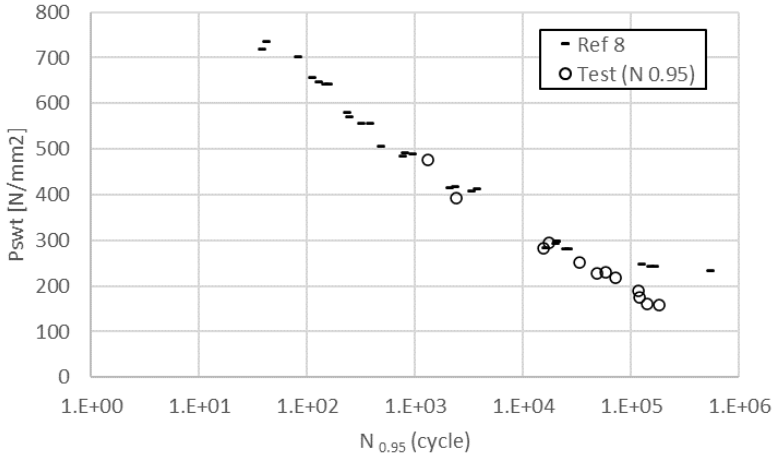

Figure 11: Relationship between product of maximum stress by strain amplitude and fatigue cycles

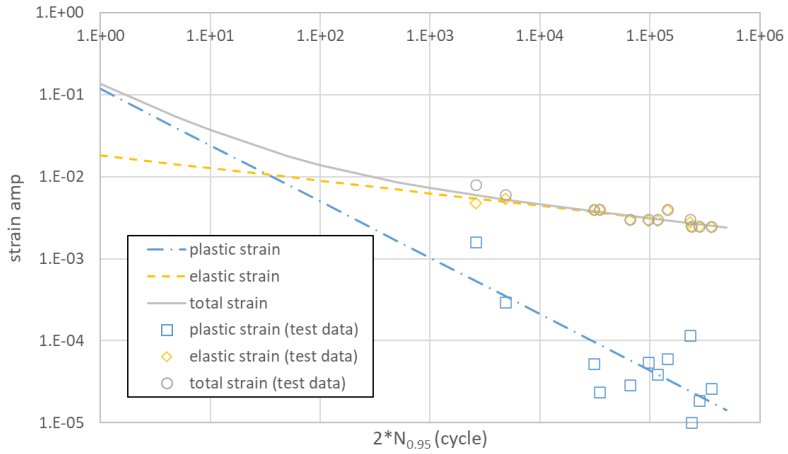

Figure 12: Relationship between strain amplitude and fatigue cycles

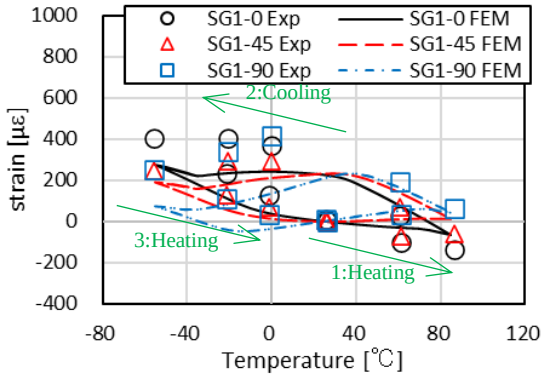

(a) Elastic strain at gauge 1

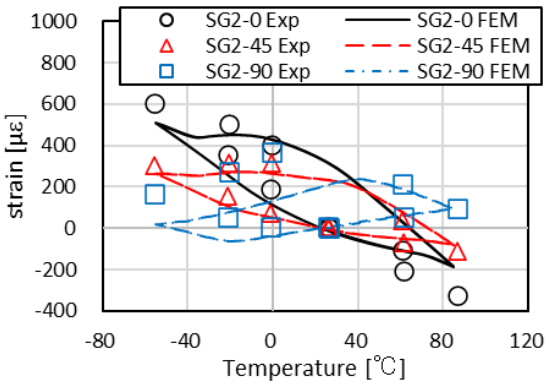

(b) Elastic strain at gauge 2

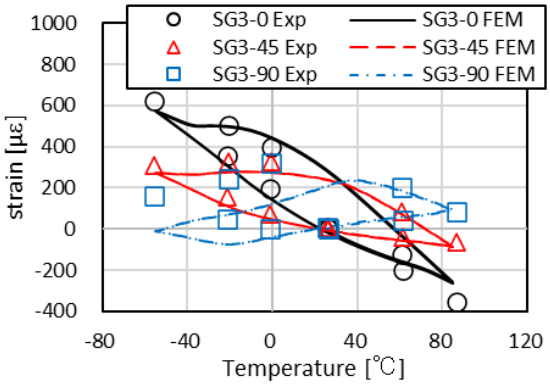

(c) Elastic strain at gauge 3

Figure 13: Hysterisis of elastic strain against temperature

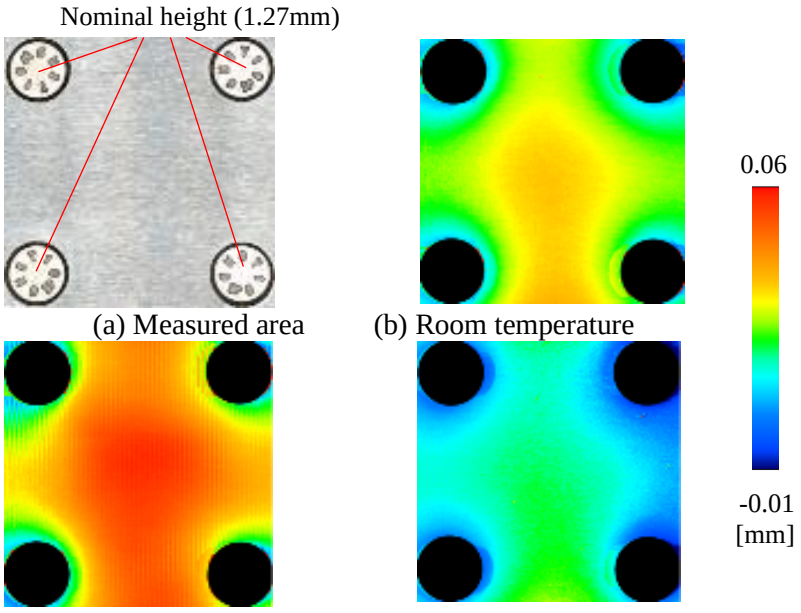

(a) Measured area (b) Room temperature

(c) About 85 degrees Celsius (d) About -55 degrees Celsius

Figure 14: Out of plane deformation of the Aluminium plate (From fastener head)

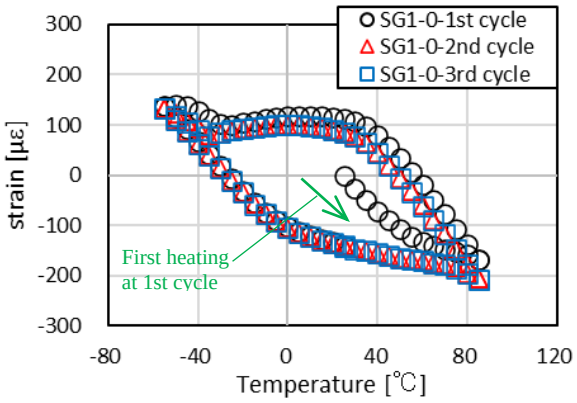

Figure 15: Strain change during temperature cycle (SG1 0 deg) obtained by FEM

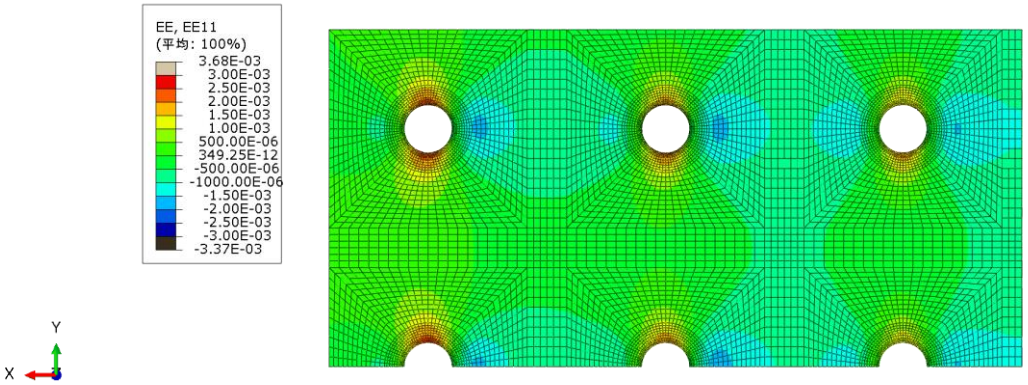

(a) 85 degrees Celsius

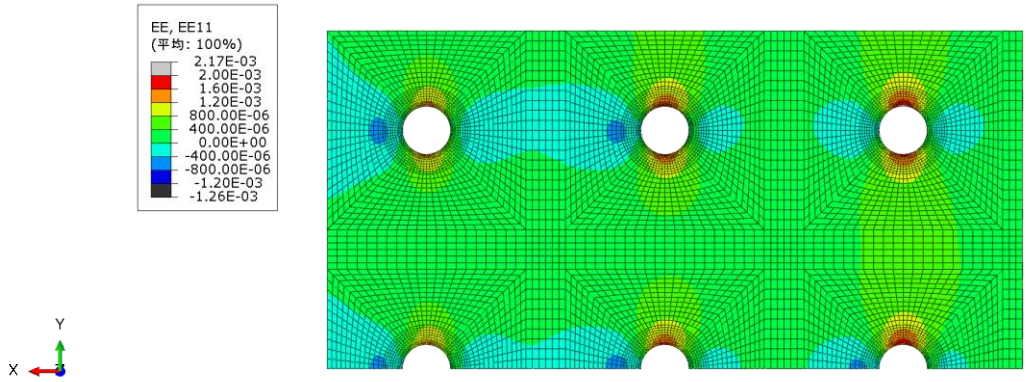

(b) -55 degrees Celsius

Figure 16: Elastic strain distribution (along x-direction) on Aluminium plate at z=2.28mm

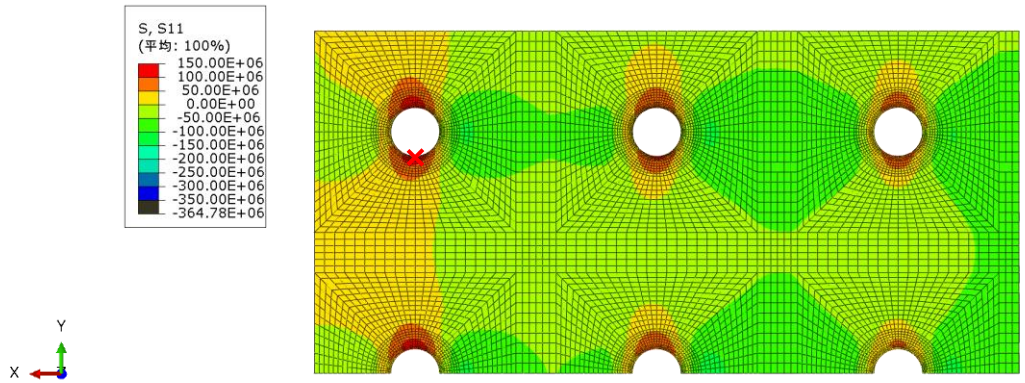

(a) 85 degrees Celsius

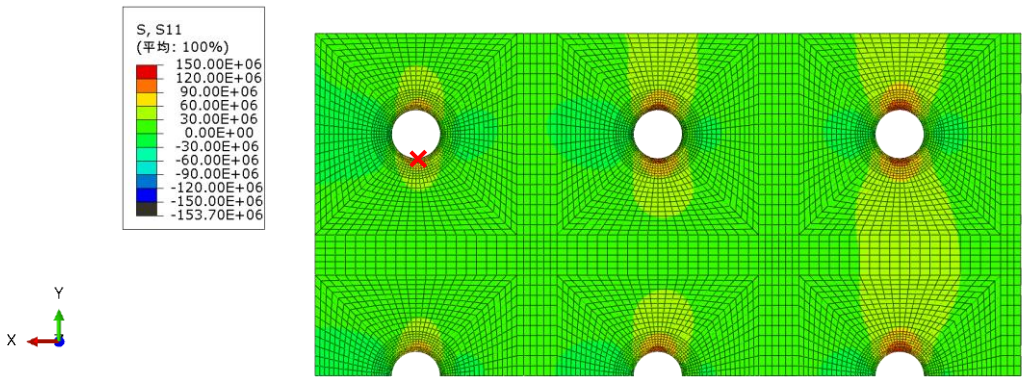

(b) -55 degrees Celsius

Figure 17: Stress distribution (along x-direction) on Aluminium plate at z=2.28mm

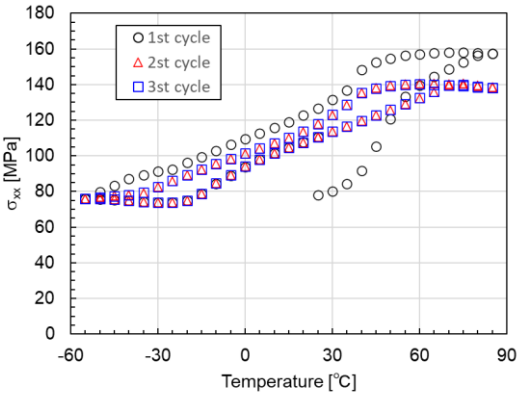

Figure 18: Stress variation at fastener hole marked in figure 17